International Journal of Nanomedicine

Dovepress
open access to scientific and medical research

Open Access Full Text Article

ORIGINAL RESEARCH

Enhanced photodynamic leishmanicidal activity of hydrophobic zinc phthalocyanine within archaeolipids containing liposomes

This article was published in the following Dove Press journal:
International Journal of Nanomedicine
10 July 2014
Number of times this article has been viewed

Ana Paula Perez[1]
Agustina Casasco[2]
Priscila Schilrreff[1]
Maria Victoria Defain Tesoriero[1,3]
Luc Duempelmann[1]
Maria Julia Altube[1]
Leticia Higa[1]
Maria Jose Morilla[1]
Patricia Petray[2]
Eder L Romero[1]

[1]Programa de Nanomedicinas, Departamento de Ciencia y Tecnología, Universidad Nacional de Quilmes, [2]Servicio de Parasitología y Enfermedad de Chagas, Hospital de Niños Ricardo Gutiérrez, [3]Unidad Operativa Sistemas de Liberación Controlada, Centro de Investigación y Desarrollo en Química, Instituto Nacional de Tecnología Industrial (INTI), Buenos Aires, Argentina

Abstract: In this work, the in vitro anti-*Leishmania* activity of photodynamic liposomes made of soybean phosphatidylcholine, sodium cholate, total polar archaeolipids (TPAs) extracted from the hyperhalophile archaea *Halorubrum tebenquichense* and the photosensitizer zinc phthalocyanine (ZnPcAL) was compared to that of ultradeformable photodynamic liposomes lacking TPAs (ZnPcUDLs). We found that while ZnPcUDLs and ZnPcALs (130 nm mean diameter and –35 mV zeta potential) were innocuous against promastigotes, a low concentration (0.01 μM ZnPc and 7.6 μM phospholipids) of ZnPcALs irradiated at a very low-energy density (0.2 J/cm^2) eliminated *L. braziliensis* amastigotes from J774 macrophages, without reducing the viability of the host cells. In such conditions, ZnPcALs were harmless for J774 macrophages, HaCaT keratinocytes, and bone marrow-derived dendritic cells. Therefore, topical photodynamic treatment would not likely affect skin-associated lymphoid tissue. ZnPcALs were extensively captured by macrophages, but ZnPcUDLs were not, leading to 2.5-fold increased intracellular delivery of ZnPc than with ZnPcUDLs. Despite mediating low levels of reactive oxygen species, the higher delivery of ZnPc and the multiple (caveolin- and clathrin-dependent plus phagocytic) intracellular pathway followed by ZnPc would have been the reason for the higher antiamastigote activity of ZnPcALs. The leishmanicidal activity of photodynamic liposomal ZnPc was improved by TPA-containing liposomes.

Keywords: macrophages, *Leishmania* amastigotes, Zn intracellular delivery, irradiation

Introduction

Latin America represents the most important endemic area of mucosal leishmaniasis,[1] which manifests from days to years after cutaneous leishmaniasis (CL), and is known as classic mucocutaneous leishmaniasis (MCL) or espundia.[2,3] MCL is a consequence of infection by New World *Leishmania* species, such as *L. braziliensis*, *L. panamensis*, *L. amazonensis*, and *L. guyanensis*.[1,4] The mucosal lesions occurring during MCL are highly destructive, severely disfiguring, and potentially deadly. MCL represents a considerable health care problem in Latin America.[5] Nowadays, leishmaniasis is largely moving towards domestic habitats,[6,7] resulting in a marked MCL-incidence rise in Europe.[8,9]

Although there are no standardized protocols for the treatment of MCL,[10] the World Health Organization recommends the use of intravenous pentavalent antimony and its derived molecules: sodium stibogluconate and meglumine antimoniate.[11] Their killing mechanism is not known, and they are effective only on the intracellular forms – the amastigotes.[12] For New World *Leishmania* species, their efficacy ranges from 30% to 90%, and sodium stibogluconate appears to be less effective than meglumine antimoniate. Their usage is limited by resistance (significant in South America)

Correspondence: Eder L Romero
Programa de Nanomedicinas, Departamento de Ciencia y Tecnología, Universidad Nacional de Quilmes, 352 Roque Saenz Peña, Bernal, Buenos Aires B1876 BXD, Argentina
Tel +54 11 4365 7100
Fax +54 11 4365 7132
Email elromero@unq.edu.ar

and cardiac, hepatic, hematic, pancreatic, and renal toxicity.[13] Intravenous pentamidine[11] possesses an efficacy of 90%–94% against *L. braziliensis*, but it is limited by resistance[12] and severe toxicity.[14,15] Other drugs of lower efficacy are miltefosine and paromomycin.[16,17] Recently, an intravenous liposomal formulation of amphotericin B (AmBisome®; Astellas Pharma, Tokyo, Japan) was shown to be effective and better tolerated than sodium stibogluconate for treatment of CL due to *L. braziliensis*.[18] Although AmBisome is claimed to be more cost effective than sodium stibogluconate treatment, the massive use of AmBisome is prohibitive for low-income people in South America. As a result of immunosuppression of human immunodeficiency virus-positive patients, kidney and heart recipients, and chronic users of corticosteroids, a serious risk of reactivation of CL in MCL form is present.[19–23] On account of such complications, treatments should be started promptly after its diagnosis, so as to prevent mucosal metastasis.

In this scenario, photodynamic therapy (PDT) is an attractive therapeutic alternative that offers the opportunity of replacing parenteral administrations of leishmanicidal agents by the topical route. In PDT, photosensitizers (PS) are excited by light to produce cytotoxic reactive oxygen species (ROS) in the presence of oxygen.[24] PDT has been widely used to eliminate diseased cells or pathogens, and has been employed with variable outcomes in experimental and clinical settings against CL.[25] PDT could avoid the problem of drug resistance, since the generated ROS could target multiple sites on the parasite. Currently, four main classes of PS – porphyrin derivatives, chlorins, porphycenes, and phthalocyanines – have been approved by the US Food and Drug Administration for the clinical treatment of cancer.[26,27] Among these, zinc phthalocyanine (ZnPc) exhibit a high photodynamic effect, as it possesses a diamagnetic Zn(II) central metal ion whose *d*-shell is fully occupied, by which the yield of triplet excited state and the long life essential for the generation of ROS becomes high.[28] Moreover, ZnPc has a large absorption cross section of light at the tissue-penetrating spectral range of 650–900 nm.[28,29]

In the particular case of CL, the clinically relevant stage of the parasites are the intracellular amastigotes within phagolysosomes in dermal macrophages. Since the singlet oxygen has a radius of destruction of ~10–55 nm,[30] the phagolysosomal location of parasites could shield them from ROS generated in a distant site of the host cell. The subcellular targeting of PS depends on their chemical structure and significantly affects photodynamic properties. For example, mitochondrial localization has been observed for hydrophobic PS, such as ZnPc, chloroaluminum phthalocyanine (ClAlPc), and protoporphyrin IX (PpIX),[31,32] in contrast to hydrophilic cationic phthalocyanines localized preferentially within the lysosomes in some cancer cells.[33,34] Therefore, a strategy leading to target PS to the phagolysosomal machinery of the infected host cells could improve photodynamic activity against CL/MCL.

With the idea of a further topical treatment, we had already shown that in vitro activity of a hydrophobic ZnPc ([tetrakis{2,4-dimetil-3-pentyloxi}-phthalocyaninate]zinc[II]) against *L. braziliensis* significantly improved when loaded in ultradeformable liposomes (UDLs; highly deformable liposomes made of phospholipids [PLs] plus such edge activators as sodium cholate, Tween 80, or Span 80).[35] In particular, these liposomes increased from 20% to 100% the antipromastigote activity and from 30% to 60% the antiamastigote activity (AA) of ZnPc, independently of irradiation. The increased AA of these UDLs was presumably due to their phagocytic uptake by the infected host cells. We later modified the UDL bilayer to get liposomes for topical application that were more extensively taken up by phagocytic cells than UDLs themselves; these improved liposomes were dubbed ultradeformable archaeosomes (UDAs). The archaeosomes (ARCs) are vesicles made of total polar archaeolipids (TPAs) extracted from the hyperhalophile archaea *Halorubrum tebenquichense*. TPAs are a mixture of *sn*-2,3-glycerol ethers with polyisoprenoid chains, where phosphatidylglycerophosphate methyl ester and sulfated diglycosyl diphytanylglycerol diether (S-DGD-5) are the most abundant lipids. To prepare UDAs, half of the soybean phosphatidylcholine (SPC) of UDLs is replaced by TPAs at the ratio SPC:TPAs:sodium cholate (3:3:1 w:w). The UDAs were successfully used as antigen carriers for topical vaccination, because of their deep skin penetration and higher phagocytic uptake than UDLs, improving the antigen delivery to skin antigen-presenting cells.[36] We hypothesized that TPAs containing liposomes could be used to increase the targeted delivery of ZnPc to macrophages to a higher extent than UDLs. Therefore, in this work, a commercial hydrophobic ZnPc was loaded into TPAs containing liposomes, and its in vitro leishmanicidal activity was compared to that of ZnPc loaded in UDLs on macrophages infected with *L. braziliensis* amastigotes.

Materials and methods

Materials

SPC (Phospholipon® 90 G, purity >90%) was a gift from Lipoid (Ludwigshafen, Germany). Sodium cholate (NaChol), 1,2-dimyristoyl-*sn*-glycero-3-phosphoethanolamine-*N*-(Lissamine™ [Thermo Fisher Scientific, Waltham, MA, USA] rhodamine B sulfonyl) (Rh-PE), ZnPc, mannan from *Saccharomyces cerevisiae*, 3-(4,5-dimethylthiazol-2-yl)-2,5-diphenyl

tetrazolium bromide (MTT), and Schneider's Insect Medium were from Sigma-Aldrich (St Louis, MO, USA). 5-(and-6)-chloromethyl-2′,7′-dichlorodihydrofluorescein diacetate, acetyl ester (carboxy-H_2DCFDA; Molecular Probes, Eugene, Oregon, USA), Roswell Park Memorial Institute (RPMI) 1640 and Modified Eagle's Medium (MEM) were from Gibco®, Life Technologies (New York, USA). Fetal calf serum (FCS), antibiotic/antimycotic solution (penicillin 10,000 IU/mL, streptomycin sulfate 10 mg/mL, amphotericin B 25 µg/mL), glutamine, and trypsin/ethylenediaminetetraacetic acid were from PAA Laboratories GmbH (Pasching, Austria). Murine recombinant granulocyte-macrophage colony-stimulating factor was obtained from Pepro Tech (Rocky Hill, NJ, USA). Complete RPMI (comp-RPMI) was prepared with RPMI 1640, 10% FCS, 5.5×10^{-5} M 2-mercaptoethanol from Sigma-Aldrich, and an antibiotic/antimycotic solution. Dendritic cell RPMI (DC-RPMI) was prepared with comp-RPMI plus 20 ng/mL of murine recombinant granulocyte-macrophage colony-stimulating factor. All other chemicals and reagents were of analytical grade.

Archaebacteria growth, extraction, and characterization of total polar lipids

Halorubrum tebenquichense Archaea, isolated from soil samples of Salina Chica, Península de Valdés, Chubut, Argentina was grown in 8 L batch cultures in basal medium supplemented with yeast extract and glucose.[37] Cultures were monitored by absorbance at 660 nm and harvested in the late stationary phase for storage as frozen cell pastes.

Total lipids were extracted from frozen and thawed biomass using the Bligh and Dyer method modified for extreme halophiles, and the TPA fraction was collected by precipitation from cold acetone.[38] Between 90 mg and 120 mg TPAs were isolated from each culture batch. The reproducibility of each TPA-extract composition was routinely screened by phosphate content[39] and electrospray-ionization mass spectrometry, as described in Higa et al.[36]

Liposome preparation

Conventional liposomes (made of SPC), ARCs (made of TPAs), UDLs (made of SPC:NaChol, 6:1 w:w), and UDAs (made of TPAs:SPC:NaChol, 3:3:1 w:w:w) were prepared by the thin-film hydration method. To that end, appropriate amounts of lipids were dissolved in chloroform (SPC) or chloroform:methanol (1:1 vol:vol) (TPAs and NaChol) and mixed in round bottom flasks. Solvents were rotary-evaporated at 40°C, and the resultant lipid films flushed with N_2 and hydrated with aqueous-phase (10 mM Tris-HCl buffer plus 0.9% w/vol NaCl, pH 7.4) buffer up to a final concentration of 43 mg of phospholipids/mL. The liposomal suspensions were sonicated (45 minutes with a bath-type sonicator, 80 W, 40 KHz) and extruded 15 times through three stacked 0.2 µm, 0.1 µm, and 0.1 µm pore polycarbonate filters using a 100 mL Thermobarrel extruder (Northern Lipids, Burnaby, Canada).

To prepare liposomes containing ZnPc, ZnPc was dissolved in dimethylformamide at 0.5 mg/mL, and 170 µL was added to the organic solution of lipids to reach 2 mg ZnPc/g phospholipids (2.5 mmol ZnPc/mol phospholipids), and liposomes were prepared as stated earlier. To prepare Rh-PE-labeled liposomes, Rh-PE was dissolved in chloroform and 12.5 nmol was added to the organic solution of lipids (nearly 2,800:1 w:w phospholipids:Rh-PE); liposomes were prepared as stated earlier.

Liposome characterization

PLs were quantified by a colorimetric phosphate microassay,[39] whereas ZnPc was quantified by absorbance at 667 nm upon complete disruption of one volume of liposomal suspension in 9 volumes of ethanol. Size and zeta potential were determined by dynamic light scattering and phase-analysis light scattering, respectively, using a Zetasizer Nano (Malvern Instruments, Malvern, UK).

The deformability value (D) of the liposomes was calculated according to Van den Bergh[40] as $D = J\ (rv/rp)^2$, where J is the rate of penetration through a permeability barrier, rv is the size of vesicles after extrusion and rp is the pore size of the barrier. To measure J, vesicles were extruded through two stacked 50 nm (rp) membranes at 0.8 MPa using the Thermobarrel extruder (Northern Lipids, Burnaby, Canada). Extruded volume was collected every minute for 15 minutes, PLs were quantified in each fraction, and J was calculated as the area under the curve of the plot of PLs recovered as a function of time. The average vesicle diameter after extrusion (rv) was measured by dynamic light scattering.

Cells and parasites

J774 and HaCat cells

Immortalized murine BALsB/c monocyte/macrophage J774 and human keratinocytes (HaCaT cells), supplied by Dr Salvatierra of the Fundación Instituto Leloir (Buenos Aires, Argentina), were routinely cultured in RPMI 1640 or MEM supplemented with 10% FCS, 100 IU/mL penicillin, 100 µg/mL streptomycin, and 2 mM glutamine at 37°C in 5% CO_2 and 95% humidity.

Bone marrow-derived dendritic cells

Bone marrow-derived DCs were obtained as described previously.[41] Briefly, cells obtained from femurs and tibias

of mice were resuspended at 1×10^6 cells/mL in DC-RPMI. The culture medium was refreshed at 48-hour intervals for 6 days by repeating the same procedure. The plates were gently swirled to remove nonadherent granulocytes without dislodging clusters of developing DCs that were loosely attached to firmly adherent macrophages. Then, 80% of the media was aspirated and removed. Fresh DC-RPMI was added very slowly to avoid disrupting the clusters. At day 8, the cell aggregates were harvested by trypsinization for 5 minutes, followed by centrifugation as mentioned earlier and overnight subculture at 3×10^5 cells/mL in comp-RPMI. The subcultures were fed at 48-hour intervals from days 10 to 14 with comp-RPMI. At days 10–14 of culture, cells were tested for specific markers. When more than 60% of the loosely adherent cells expressed the CD11c marker, they were considered ready to use.

Leishmania parasites

L. braziliensis promastigotes (strain HOM/BR75/M2903), supplied by Dr Mónica Esteva from the Instituto Nacional de Parasitologia Dr Mario Fatala Chabén (Buenos Aires, Argentina), were cultured at 26°C in Schneider's Insect Medium supplemented with 10% FCS, 100 IU/mL penicillin, 100 µg/mL streptomycin, and 2 mM glutamine. Growth curves of the parasite were performed, and promastigotes at the stationary phase were used for macrophage infection.

Uptake of liposomes by macrophages

The uptake of Rh-PE-labeled liposomes by macrophages was analyzed by flow cytometry. J774 cells seeded at a density of 3.5×10^5 cells per well onto six-well microplates were grown for 24 hours at 37°C. The medium was replaced with fresh MEM with 5% FCS containing Rh-PE-labeled liposomes, ARCs, UDLs, and UDAs at 0.5 mM PLs, and cells were incubated for 1, 3, and 5 hours at 37°C. After each incubation time, the medium was removed, cells were washed with phosphate-buffered saline (PBS; pH 7.4), and harvested by trypsinization. Cells were fixed in 1% formaldehyde at 4°C. Cells were washed, suspended in PBS, and a total of 1×10^5 cells were analyzed by flow cytometry (BD FACSCalibur™; BD Biosciences, San Jose, CA, USA). Data were analyzed using WinMDI 2.9 software (Microsoft, Redmond, WA, USA).

Cytotoxicity on keratinocytes, macrophages, and dendritic cells

HaCaT and J774 cells and DC were seeded at a density of 5× and 9×10^4 cells per well, respectively, onto 96-well flat-bottom plates and grown for 24 hours at 37°C. Then, the medium was replaced by 100 µL of fresh medium with 5% FCS containing 0.01 µM and 0.1 µM of free or liposomal ZnPc (corresponding to 7.6–5.2 µM PLs and 76–52 µM PLs). After 24-hour incubation at 37°C, suspensions were removed; cells were washed with PBS, and fresh MEM with 5% FCS was added. Cells were irradiated for 15 minutes with a halogen lamp (7748S 250 W; Philips, Amsterdam, the Netherlands) that provided an average irradiance of 0.22 mW/cm^2 (measured with a SpectroSense2 light meter with an SKR 110/SS2 sensor at 660 nm; Skye Instruments, Powys, UK) at a distance of 26 cm from the plates positioned perpendicularly to the center of the lamp. Illumination time of 15 minutes provided energy fluency of 0.2 J/cm^2. Control cells were maintained without irradiation. After irradiation, cells were incubated for 24 hours at 37°C, and then the medium was removed and replaced by 0.5 mg/mL of MTT. After 4 hours' incubation, the MTT solution was removed, the insoluble formazan crystals were dissolved in dimethyl sulfoxide, and absorbance was measured at 570 nm in a microplate reader. The viability of cells was expressed as a percentage of the viability of cells grown in medium.

Antipromastigote activity

L. braziliensis promastigotes (1×10^6) were incubated with 0.01 µM and 0.1 µM of free or liposomal ZnPc at 26°C in Schneider's Insect Medium. After 24 hours' incubation at 26°C, suspensions were removed; parasites were washed with PBS, fresh Schneider's Insect medium with 5% FCS was added, and parasites were irradiated with 0.2 J/cm^2. Control parasites were maintained without irradiation. After irradiation, parasites were incubated for 24 hours at 26°C, and then parasite viability was measured by MTT assay.

Antiamastigote activity

J774 cells were seeded at a density of 2×10^4 cells per well in eight-well culture-chamber slides (Nunc™ Lab-Tek™; Thermo Fisher Scientific), and grown for 24 hours at 37°C. Thereafter, J774 cells were infected for 4 hours with *L. braziliensis* promastigotes at a 1:6 macrophages:promastigotes ratio, and then extracellular parasites were removed by gently washing. The medium was replaced by 100 µL of fresh MEM with 5% FCS containing 0.01 µM and 0.1 µM of free or liposomal ZnPc. Cells were incubated for an additional 4 hours, and then irradiated with 0.2 J/cm^2. Control cells were maintained without irradiation. After 24 hours, cells were washed with PBS, fixed with methanol, and stained with Giemsa. The number of amastigotes/100 cells was determined by counting at least 300 cells in triplicate cultures in each experimental condition by using light microscopy.

Untreated infected macrophages were used as controls. Antiamastigote activity was expressed as: %AA = (1–[{number of amastigotes/100 treated cells}/{number of amastigotes/100 untreated cells} × 100]).

ZnPc delivery to macrophages

The uptake of free or liposomal ZnPc by J774 cells was analyzed by flow cytometry. Cells were seeded at a density of 1.5×10^5 cells per well onto 24-well plates and grown for 24 hours at 37°C. Then, the medium was replaced by 250 µL of fresh MEM with 5% FCS containing 0.01 µM of free or liposomal ZnPc (5.2–7.6 µM PL). After 24 hours' incubation at 37°C, suspensions were removed, cells were washed with and suspended in PBS, and a total of 2×10^4 cells were analyzed by flow cytometry.

Competition assay

J774 cells seeded at a density of 1.5×10^5 cells per well onto 24-well microplates were grown for 24 hours at 37°C. The medium was replaced with fresh MEM with 5% FCS containing 4 mg/mL mannan for 30 minutes. Then, 0.1 µM of liposomal ZnPc (corresponding to 76–52 µM PLs) was added and incubated for another 1 hour at 37°C. Cells were washed with PBS (pH 7.4) and harvested by trypsinization. Cells were suspended in PBS, and a total of 2×10^4 cells were analyzed by flow cytometry.

Measurement of reactive oxygen species

Carboxy-H_2DCFDA dye was used to study intracellular ROS generation in J774 cells. Carboxy-H_2DCFDA is a chemically reduced, acetylated form of fluorescein used as an indicator for ROS in cells. This nonfluorescent molecule is readily converted to a green fluorescent form when the acetate groups are removed by intracellular esterases and oxidation (by the activity of ROS) occurs within the cell. Cells were seeded at a density of 1.5×10^5 cells per well onto 24-well plates and grown for 24 hours at 37°C. Then, the medium was replaced by 250 µL of fresh MEM with 5% FCS containing 0.01 µM and 0.1 µM of free or liposomal ZnPc. After 4 hours' incubation at 37°C, suspensions were removed, cells were washed with PBS, and the medium was replaced by fresh MEM with 5% FCS. Cells were irradiated with 0.2 J/cm^2. Control cells were maintained without irradiation. After irradiation, cells were incubated for 30 minutes at 37°C, and then the medium was removed and replaced by 10 µM of carboxy-H_2DCFDA in PBS. After 30 minutes' incubation, the solution was removed, cells were washed in and suspended in PBS, and a total of 2×10^4 cells were analyzed by flow cytometry. As a positive control, intracellular ROS production was induced by the addition of 2.5 µM H_2O_2 for 30 minutes before the addition of carboxy-H_2DCFDA.

Statistical analysis

Group means of results with two variables were evaluated by two-way analysis of variance (ANOVA) followed by Bonferroni correction, and results with one variable were evaluated by one-way ANOVA followed by Tukey's test to compare individual groups using Prism 4.0 software (GraphPad Software, La Jolla, CA, USA). Significance levels are described in figure legends.

Results

Characterization of liposomes

The main structural features of void and ZnPc-containing liposomes are shown in Table 1. We found that the incorporation of ZnPc into the UDL bilayer did not significantly modify its deformability. However, the insertion of ZnPc into the UDA bilayer considerably reduced its deformability to the order of that of conventional liposomes. It is expected that a relative absence of postextrusion size reduction will be found, as long as the bilayers are highly deformable, as occurred with UDLs and UDAs, whose mean size was reduced by 0 and 15%, respectively. On the other hand, a significant size reduction upon extrusion is expected for poorly deformable bilayers

Table 1 Structural characteristics of void and ZnPc containing liposomes. Values given are mean values of three different batches ± standard deviation of the mean

Sample	Mean size (nm) (polydispersity index)	Zeta potential (mV)	Mean size, post-deformability test (nm)	Deformability (*D*)	mmol ZnPc/mol phospholipids
Ls	109±5 (0.103)	−10±3	62±6	765±267	–
UDLs	110±2 (0.242)	−12±2	109±2	3,882±291	–
UDAs	130±1 (0.241)	−35±4	110±2	4,064±365	–
ZnPcUDLs	112±10 (0.10)	−11±4	89±1	3,391±393	1.9±0.4
ZnPcALs	131±19 (0.13)	−35±1	96±1	425±130	1.4±0.7

Abbreviations: Ls, conventional liposomes; UDLs, ultradeformable liposomes; UDAs, ultradeformable archaeosomes; ZnPcUDLs, ZnPc containing ultradeformable liposomes; ZnPcALs, ZnPc and archaeolipids containing liposomes.

such as liposomes and ZnPcALs, whose mean size was reduced by 43% and 27%, respectively. Another factor contributing to *D* is the flux (J) measured as the amount of filtered phospholipids/time. We found that 85% of the total ZnPcUDL phospholipids were filtered in the first 15 minutes, versus only 10% for ZnPcALs. Therefore, we will refer to these liposomes as ZnPcALs (instead of ZnPcUDAs), where ALs means archaeolipids containing liposomes.

Uptake of liposomes by macrophages

The phagocytic uptake of ARCs (nondeformable vesicles made of TPAs), UDAs (TPA-containing deformable vesicles), UDLs, and liposomes was compared. We found that ARCs and UDAs were extensively taken up, while the uptake of UDLs and liposomes was negligible (Figure 1). No significant difference was found between the uptake of UDAs or ARCs, their extensive phagocytosis likely related to the TPA content and not to their bilayer deformability. Therefore, despite not being deformable, ZnPcALs remained as suitable candidates as leishmanicidal liposomes to be taken up by infected macrophages.

Cytotoxicity on keratinocytes, macrophages, and dendritic cells

Neither ZnPc in darkness or after irradiation nor ZnPc liposomes in darkness were cytotoxic on all cell types. After irradiation, 0.01 μM ZnPcUDLs and ZnPcALs were also innocuous on all cell types; however, at 0.1 μM, both decreased by 60% the viability of HaCaT cells (Figure 2A), and ZnPcALs decreased by 40% the viability of J774 cells

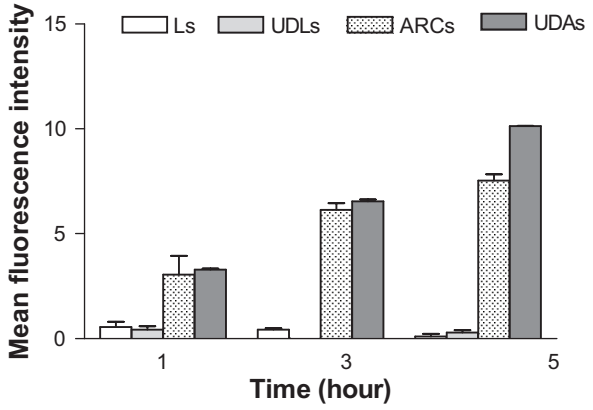

Figure 1 Uptake of Rh-PE-labeled liposomes by J774 cells as a function of time.
Notes: J774 cells were incubated with Rh-PE-Ls, Rh-PE-UDLs, Rh-PE-ARCs, and Rh-PE-UDAs at 0.5 mM phospholipids in medium containing 5% FCS. At different time points, cells were washed with phosphate-buffered saline, collected, fixed, and analyzed by flow cytometry (BD FACSCalibur™; BD Biosciences, San Jose, CA, USA).
Abbreviations: Rh-PE, dimyristoyl phosphoethanolamine-*N*-(Lissamine rhodamine B sulfonyl); Ls, conventional liposomes; UDLs, ultradeformable liposomes; ARCs, archaeosomes; UDAs, ultradeformable archaeosomes; FCS, fetal calf serum.

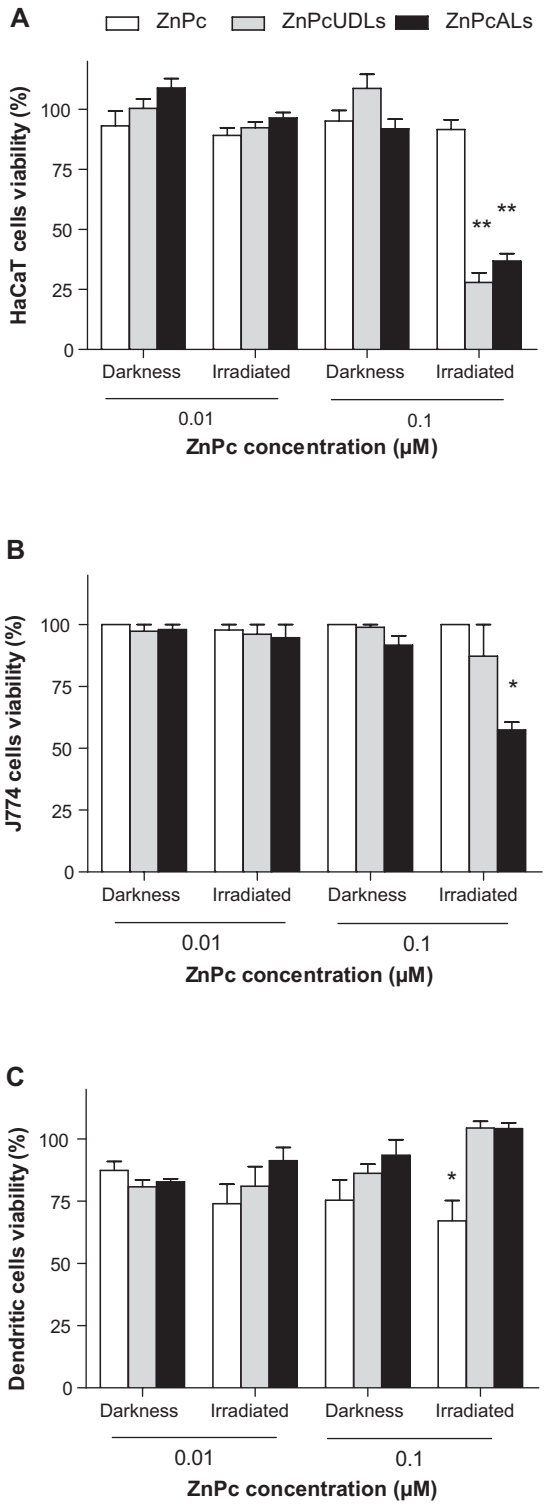

Figure 2 Cytotoxicity of free and liposomal ZnPc on mammal cells in the darkness and after irradiation.
Notes: HaCaT cells (**A**), J774 cells (**B**), and dendritic cells (**C**) were incubated with 0.01 μM and 0.1 μM of ZnPc, ZnPcUDLs, and ZnPcALs for 24 hours in medium containing 5% FCS. Half the cells were kept in the darkness, and half were irradiated. After irradiation, cells were incubated for 24 hours in growth medium. Cell survival was determined by the 3-(4,5-dimethylthiazol-2-yl)-2,5-diphenyltetrazolium bromide assay. Values represent means ± standard deviation (n=3). $^{**}P<0.01$; $^{*}P<0.05$.
Abbreviations: ZnPc, zinc phthalocyanine; ZnPcUDLs, ZnPc containing ultradeformable liposomes; ZnPcALs, ZnPc and archaeolipids containing liposomes; FCS, fetal calf serum.

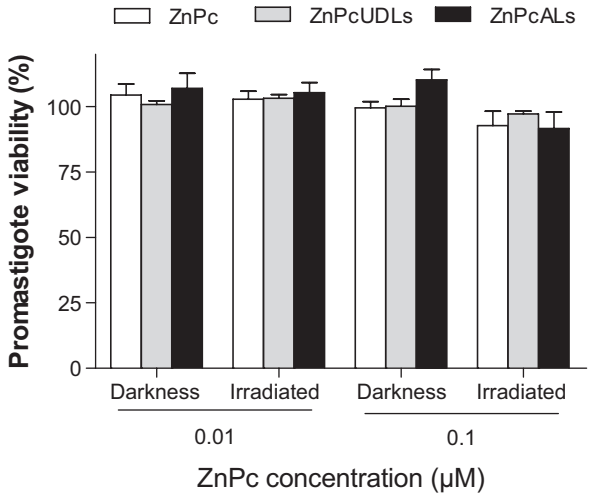

Figure 3 Cytotoxicity of free and liposomal ZnPc on *Leishmania braziliensis* promastigotes in the darkness and after irradiation.

Notes: *L. braziliensis* promastigotes were incubated with 0.01 μM and 0.1 μM of ZnPc, ZnPcUDLs, and ZnPcALs for 24 hours in Schneider's Insect Medium (Sigma Aldrich, St Louis, MO, USA) at 26°C. Half the parasites were kept in darkness, and half were irradiated. After irradiation, parasites were incubated for 24 hours in growth medium. Cell survival was determined by the 3-(4,5-dimethylthiazol-2-yl)-2,5-diphenyltetrazolium bromide assay. Values represent means ± standard deviation (n=3).

Abbreviations: ZnPc, zinc phthalocyanine; ZnPcUDLs, ZnPc containing ultradeformable liposomes; ZnPcALs, ZnPc and archaeolipids containing liposomes.

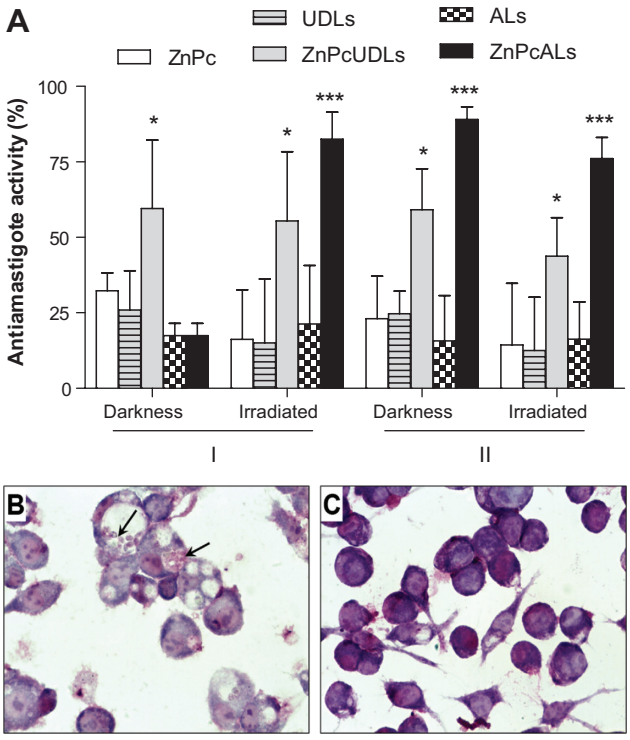

Figure 4 Antiamastigote activity of free or liposomal ZnPc in the darkness and after irradiation.

Notes: (**A**) J774 cells previously infected with *Leishmania braziliensis* promastigotes were incubated with 0.01 μM (I) and 0.1 μM (II) of ZnPc, ZnPcUDLs, and ZnPcALs, and with void liposomes (UDLs and ALs at the phospholipid concentrations 7.6–5.2 [I] μM and 76–52 [II] μM) for 4 hours in medium containing 5% fetal calf serum. Half the cells were kept in darkness, and half were irradiated. After irradiation, cells were incubated for 24 hours in growth medium. Then cells were fixed with methanol and stained with Giemsa (Merck, New Jersey, USA). The number of amastigotes/100 cells was determined by counting at least 300 cells in three different experiments, and antiamastigote activity was calculated. (**B**,**C**) Optical microscopy of infected J774 cells incubated with 0.01 μM ZnPc (**B**) and 0.01 μM ZnPcALs (**C**), both taken 24 hours after irradiation. Arrows points to intracellular amastigotes. *$P<0.05$; ***$P<0.001$.

Abbreviations: ZnPc, zinc phthalocyanine; ZnPcUDLs, ZnPc containing ultradeformable liposomes; ZnPcALs, ZnPc and archaeolipids containing liposomes; UDLs, ultradeformable liposomes; ALs, archaeolipids containing liposomes.

(Figure 2B). ZnPcUDLs and ZnPcALs were not cytotoxic on DCs (Figure 2C) in darkness or after irradiation, indicating therefore a lower sensitivity to liposomal PDT than macrophages and keratinocytes.

Antipromastigote activity

Neither ZnPc nor ZnPc liposomes reduced the viability of *L. braziliensis* promastigotes in darkness or after irradiation (Figure 3).

Antiamastigote activity

Interestingly, we found a basal concentration- and irradiation-independent AA of around 25% for UDLs, UDAs, and ZnPc. Similarly, the 50%–60% AA of ZnPcUDLs was concentration- and irradiation-independent as well (Figure 4A). The 85%–90% AA of ZnPcALs at 0.1 μM ZnPc was also irradiation-independent. However, the 15% AA of ZnPcALs at 0.01 μM ZnPc in darkness significantly increased to near 90% after irradiation. Optical microscopy of infected macrophages treated with 0.01 μM ZnPc (Figure 4B) and 0.01 μM ZnPcALs (Figure 4C) after irradiation showed the preservation of intact morphology of macrophages, together with a reduction in the number of amastigotes per macrophage.

ZnPc delivery to macrophages

The amount of ZnPc delivered by ZnPcALs to J774 cells was quantified by flow cytometry of the fluorescent ZnPc, and was 2.5-fold higher than that delivered by ZnPcUDLs or ZnPc (Figure 5A). Remarkably, the uptake of ZnPcALs and not of ZnPcUDLs was strongly reduced in the presence of the mannose polysaccharide yeast mannan (Figure 5B).

Production of ROS

Only macrophages treated with 0.1 μM ZnPcALs generated measurable levels of ROS in an irradiation-independent fashion (Figure 6).

Discussion

In this work, based on the hypothesis that TPAs containing liposomes could improve ZnPc delivery to infected macrophages, the in vitro leishmanicidal activity of ZnPcALs was compared to that of ZnPcUDLs and free ZnPc on macrophages infected with *L. braziliensis*.

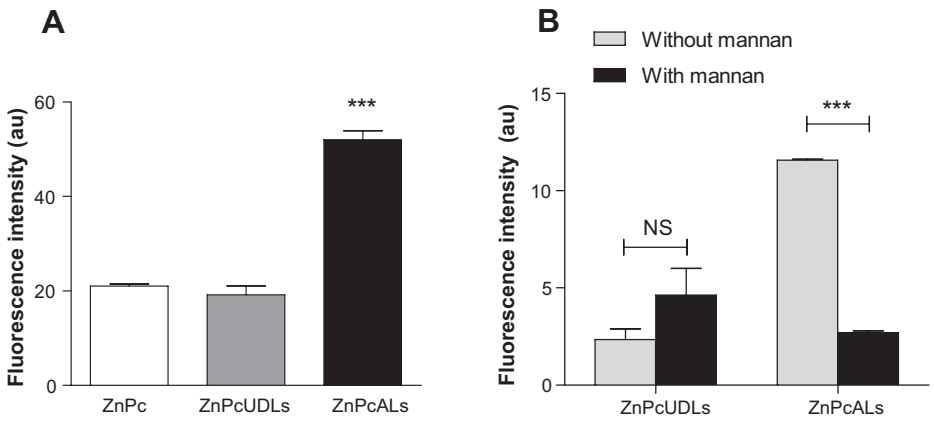

Figure 5 Uptake of liposomal ZnPc by J774 cells.
Notes: (**A**) J774 cells were incubated with 0.01 μM of ZnPc, ZnPcUDLs, and ZnPcALs for 24 hours in medium containing 5% fetal calf serum (FCS). Then, cells were washed with phosphate-buffered saline (PBS), suspended in PBS, and analyzed by flow cytometry (BD FACSCalibur™; BD Biosciences, San Jose, CA, USA). (**B**) J774 cells were preincubated with 4 mg/mL mannan for 30 minutes in medium containing 5% FCS, then 0.1 μM of ZnPcUDLs and ZnPcALs were added and incubated for another hour at 37°C. Then, cells were washed with PBS, suspended in PBS, and analyzed by flow cytometry. Values represent mean ± standard deviation (n=3). ***$P<0.001$.
Abbreviations: ZnPc, zinc phthalocyanine; ZnPcUDLs, ZnPc containing ultradeformable liposomes; ZnPcALs, ZnPc and archaeolipids containing liposomes; NS, not significant.

First we found that insertion of ZnPc into the UDA bilayer considerably reduced its deformability. Bilayer deformability depends on the mixing/demixing of edge activators (EAs; hydrophilic detergents, such as sodium cholate, deoxycholate, or Tween 80) as a response to mechanical deformation stress.[42,43] However, the lateral mobility of foreign molecules dissolved within polyisoprenoid lipids rich in sugar, such as TPA bilayers, is low. In a previous work, we observed that the addition of EAs to pure TPA bilayers does not lead to highly deformable liposomes, due to the impaired lateral mobility (mixing/demixing) of EAs in TPAs. In order to make TPA bilayers highly deformable, a minimal proportion of SPC is required at 3:1:3 w:w SPC:NaChol:TPAs. Below that SPC threshold, the presence of EAs is insufficient to make the TPA bilayer highly deformable. SPC is therefore unavoidable, since the mixing of EAs occurs after the TPA is diluted in a given amount of SPC.[44] It is likely, therefore, that the insertion of hydrophobic ZnPc within the TPA–SPC mixture interfered with EA demixing, decreasing its deformability.

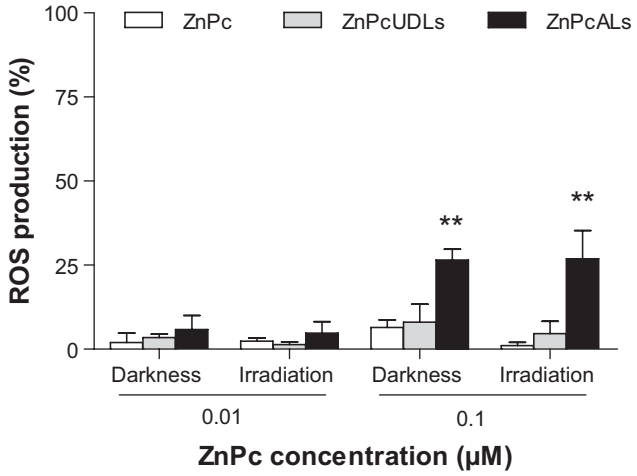

Figure 6 Reactive oxygen species (ROS) production of J774 cells after treatment with free or liposomal ZnPc in darkness and after irradiation.
Notes: J774 cells were incubated with 0.01 μM and 0.1 μM of ZnPc, ZnPcUDLs, and ZnPcALs for 4 hours in medium containing 5% fetal calf serum. Half the cells were kept in darkness, and half were irradiated. After irradiation, cells were incubated for 30 minutes at 37°C, and then medium was removed and replaced by 10 μM of (5-and-6)-chloromethyl-2′,7′-dichlorodihydrofluorescein diacetate, acetyl ester in phosphate-buffered saline (PBS). Then, cells were washed with PBS, suspended in PBS, and analyzed by flow cytometry (BD FACSCalibur™; BD Biosciences, San Jose, CA, USA). Values represent means ± standard deviation (n=3). **$P<0.01$.
Abbreviations: ZnPc, zinc phthalocyanine; ZnPcUDLs, ZnPc containing ultradeformable liposomes; ZnPcALs, ZnPc and archaeolipids containing liposomes.

On the other hand, we found that the intracellular ZnPc delivered to macrophages by 0.01 μM ZnPcALs was 2.5-fold higher than that delivered by ZnPcUDLs or ZnPc. We also observed that after irradiation at 0.2 J/cm^2 fluency, the AA of 0.01 μM ZnPcALs was 60% higher than with ZnPc and 35% higher than with ZnPcUDLs. Although free ZnPc or ZnPcUDLs delivered the same amount of intracellular ZnPc, the higher AA of ZnPcUDLs could be due to the different intracellular localization of ZnPc. While free ZnPc enters by diffusion,[45] ZnPcUDLs are taken up by clathrin-mediated endocytosis, the ZnPc delivered to intracellular targets being different to those by diffusion.[46] Instead, the higher AA of 0.01 μM ZnPcALs than ZnPcUDLs would be a consequence of the higher ZnPc endocytic uptake of the mannosylated liposomes following particular intracellular traffic. It was recently reported that 100 nm-diameter TPAs containing liposomes were taken up by J774 cells

by multiple pathways that included phagocytosis and clathrin- and caveolin-mediated endocytosis (Defain et al, unpublished data, 2014). The mannose receptor (MR) expressed in J774 is involved in high endocytic uptake of mannosylated ligands.[47] The uptake of ZnPcALs was strongly reduced via coadministration with mannan, indicating that internalization of ZnPcALs was mediated by the mannose receptor. The high uptake of TPAs containing liposomes, ARCs, UDAs, and ZnPcALs suggested an interaction between the sulfated mannosylated archaeolipid S-DGD-5 1-O-[α-D-mannose-(2″-SO_3H)-(1′→2′)-α-D-glucose]-2,3-di-O-phytanyl-sn-glycerol) and the MR, primarily expressed by macrophages, DCs, and some epithelial cells.[48] Remarkably, a high uptake plus the noninduction of proinflammatory cytokines are hallmarks of the interaction via MR,[49–51] and we have recently observed that despite being highly taken up, UDAs did not induce the proinflammatory cytokines tumor necrosis factor-α and interleukin 6 by J774 cells (Perez et al, unpublished data, 2014).

The PDT with 0.01 μM liposomal ZnPc resulted in toxicity to intracellular parasites, but was innocuous for host macrophages and keratinocytes. Remarkably, primary DCs – a cell type expected to be target of TPAs containing liposomes, due to their constitutive expression of MR[48] – showed surprising resistance to the liposomal PDT. This would suggest that further topical PDT would not affect the immune functions of skin-associated lymphoid tissue.

Interestingly, we found that irradiation with liposomal ZnPc significantly inhibited the survival of amastigotes inside host macrophage, cells but had no antipromastigote effect. Similar results were found for paromomycin-containing liposomes and transfersomes, where activities against intracellular *L. major* amastigotes were higher than activities against promastigotes.[52,53]

Quantitative comparisons of our results with other contributions are difficult to establish, due to the scarcity of studies on the activity of ZnPc-mediated PDT against New World leishmaniasis. Our in vitro results showed that 0.01 μM ZnPcAL-mediated PDT at 0.2 J/cm^2 was deleterious against intracellular amastigotes and kept viable macrophages, keratinocytes, and dendritic host cells. Interestingly, this was achieved at a 100-fold lower dose of PS (1.25 μM) and 75-fold lower fluency (15 J/cm^2) than we have reported before with ZnPcUDLs ([tetrakis{2,4-dimetil-3-pentyloxi}-phthalocyaninate] zinc [II]).[35] On the other hand, our results were achieved at 10^4–10^5-fold lower doses of PS (1 mM δ-aminolevulinic acid [ALA] and 1 mM PpIX) and 50–100-fold lower fluency (50–10 J/cm^2) than with ALA or PpIX, that had previously failed to eliminate intracellular *L. major* amastigotes.[54,55] With such an approach, macrophages were more sensitive than the parasites to ALA, suggesting that death of the host cells likely occurred without complete eradication of the parasites. Our results also were achieved at a 180-fold lower dose and 5.5- to eleven-fold lower fluency than with liposomal carbaporphyrin dimethyl ketal, which showed a half-maximal effective concentration of 1.8 μM against intracellular *L. amazonensis* amastigotes.[56] Finally, our results were achieved at a seven- to 15-fold higher dose than with liposomal AlPcCl, which showed half-maximal inhibitory concentrations of 1.49 and 0.69 nM against intracellular *L. panamensis* and *L. chagasi* amastigotes, respectively.[57] Nonetheless, these were similar to the half-maximal cytotoxicity concentration on macrophages (1.35 nM). This means that the uninfected macrophages were eliminated by similar (or quite a lot lower) concentration of ClAlPc than intracellular amastigotes. These kinds of results were also reported for free ALA[58] and AlPcCl.[59] In all cases, our results were achieved at 34-fold lower fluency without reducing macrophage viability.

Unfortunately, in studies that used PDT as a leishmanicidal agent, the measurement of intracellular ROS was avoided.[54–59] However, at 0.01 μM ZnPcALs, the induction of AA in response to irradiation suggested the mediation of ROS that produced below the minimal detection level of the method[60] and was lethal for intracellular amastigotes. Here, carboxy-H_2DCFDA (used to detect hydrogen peroxide; peroxyl radicals, including alkyl peroxyl and hydroperoxyl; and peroxynitrite anions in cell-free systems) showed quantitative and irradiation-independent ROS production by 0.1 μM ZnPcALs. After irradiating 0.01 μM ZnPcALs, however, no ROS were detected. The results could be interpreted as arising from a chemotoxic, concentration-dependent instead of a photodynamic activity. A partial explanation for this would lie in the fact that ROS can be produced in the dark by chemical reactions and not exclusively by photodynamic activity.

In general, the endocytic uptake of liposomes results in therapeutic effects with minimal amounts of active principle, because of selective delivery to intracellular targets. In our case, PDT with 0.01 μM ZnPcALs combined a high amount of intracellular ZnPc with a probable local generation of ROS at multiple intracellular targets by phagocytosis and clathrin- and caveolin-mediated endocytosis that was lethal for amastigotes. Our finding of a high AA of 0.01 μM ZnPC-UDLs independent of irradiation suggested the intervention of chemotoxicity and not ROS-mediated mechanisms. Similarly, Taylor et al[56] reported that the activity of liposomal carbaporphyrin dimethyl ketal on intracellular amastigotes of *L. amazonensis* was irradiation-independent, and when tested in vivo using

a hamster model of CL with *L. amazonensis*, carbaporphyrin ketals were active even in the dark. The authors suggested that the compound, once metabolized in the animal tissue, produces an active ingredient that does not seem to be photosensitive. Nonetheless, the increased AA after irradiation of 0.01 μM ZnPcALs strongly suggested the intervention of photoinduction, although our experimental setting was unable to show a ROS increment as a response to irradiation. A potential explanation would be that the intracellular delivery of 0.01 μM ZnPcALs would favor a direct and lethal attack of $^1O_2$ (undetectable by carboxy-H_2DCFDA) to the parasite lipids, nucleic acids, and proteins, resulting in minimal ROS production. The results at 0.1 μM ZnPcALs could be explained by the superimposition of phototoxicity and chemical toxicity that could also be mediated by ROS in the dark.

Finally, at 0.1 μM liposomal ZnPc in the dark, the intracellular parasites were affected, while the host cells suffered no damage. After irradiation, however, ZnPcUDLs damaged keratinocytes, while ZnPcALs damaged keratinocytes and macrophages as well. These in vitro assays would suggest that in vivo, the dosage scheme will have to be adjusted in order to achieve leishmanicidal activity, but also to avoid potential epidermal cytotoxicity.

Acknowledgments

This work was supported by CONICET PIP-2010-2012 893, Fundación Bunge y Born, the EULANEST project Nanoskin, and Secretaria de Investigaciones, Universidad Nacional de Quilmes. APP, LH, PBP, MJM, and ELR are members of the Research Career Program of CONICET.

Disclosure

The authors report no conflicts of interest in this work.

References

1. Goto H, Lindoso JAL. Current diagnosis and treatment of cutaneous and mucocutaneous leishmaniasis. *Expert Rev Anti Infect Ther*. 2010; 8:419–433.
2. World Health Organization. *Working to Overcome the Global Impact of Neglected Tropical Disease: First WHO Report on Neglected Tropical Diseases*. Geneva: WHO; 2010.
3. Aliaga L, Cobo F, Mediavilla JD, et al. Localized mucosal leishmaniasis due to *Leishmania* (*Leishmania*) *infantum* clinical and microbiologic findings in 31 patients. *Medicine (Baltimore)*. 2003;82:147–158.
4. Lessa MM, Lessa HA, Castro TWN, et al. Mucosal leishmaniasis: epidemiological and clinical aspects. *Braz J Otorhinolaryngol*. 2007;73:843–847.
5. Sabbaga AV, Tuon FF, Bacha HA, Neto VA, Nicodemo AC. Mucosal leishmaniasis current scenario and prospects for treatment. *Acta Trop*. 2008;105:1–9.
6. Garcia L, Parrado R, Rojas E, Delgado R, Dujardin JC, Reithinger R. Leishmaniases in Bolivia: comprehensive review and current status. *Am J Trop Med Hyg*. 2009;80:704–711.
7. Tedesqui VL, Calleja GN, Parra R, Pabón JP, Bóia MN, Carvalho-Costa FA. Active surveillance of American tegumentary leishmaniasis in endemic areas in rural Bolivia. *Rev Soc Bras de Med Trop*. 2012;45:30–34.
8. Ready PD. Leishmaniasis emergence in Europe. *Euro Surveill*. 2010;15:19505.
9. de Oliveira CI, Brodskyn CI. The immunobiology of *Leishmania braziliensis* infection. *Front Immunol*. 2012;3:145.
10. Strazzulla A, Cocuzza S, Pinzone MR, et al. Mucosal leishmaniasis: an underestimated presentation of a neglected disease. *Bio Med Res Int*. 2013;2013:805108.
11. David CV, Craft N. Cutaneous and mucocutaneous leishmaniasis. *Dermatol Ther*. 2009;22:491–502.
12. Amato VS, Tuon FF, Bacha HA, Neto VA, Nicodemo AC. Mucosal leishmaniasis: current scenario and prospects for treatment. *Acta Trop*. 2008;105:1–9.
13. Blum J, Desjeux P, Schwartz E, Beck B, Hatz C. Treatment of cutaneous leishmaniasis among travellers. *J Antimicrob Chemother*. 2004;53:158–166.
14. Machado PRL, Lassa H, Lessa M, et al. Oral pentoxifylline combined with pentavalent antimony: a randomized trial for mucosal leishmaniasis. *Clin Infect Dis*. 2007;44:788–793.
15. Kappagoda S, Singh U, Blackburn BG. Antiparasitic therapy. *Mayo Clin Proceed*. 2011;86:561–583.
16. Soto J, Tolado J, Valda L, et al. Treatment of Bolivian mucosal leishmaniasis with miltefosine. *Clin Infect Dis*. 2007;44:350–356.
17. Soto J, Rea J, Valderrama M, et al. Efficacy of extended (six weeks) treatment with miltefosine for mucosal leishmaniasis in Bolivia. *Am J Trop Med Hyg*. 2009;81:387–389.
18. Solomon M, Pavlotzky F, Barzilai A, Schwartz E. Liposomal amphotericin B in comparison to sodium stibogluconate for *Leishmania braziliensis* cutaneous leishmaniasis in travelers. *J Am Acad Dermatol*. 2013; 68:284–289.
19. Alrajhi AA, Saleem M, Ibrahim EA, Gramiccia M. Leishmaniasis of the tongue in a renal transplant recipient. *Clin Infect Dis*. 1998; 27:1332–1333.
20. Iborra C, Caumes E, Carriere J, Cavelier-Balloy B, Danis M, Bricaire F. Mucosal leishmaniasis in a heart transplant recipient. *Br J Dermatol*. 1998;138:190–192.
21. Chaudhry Z, Barrett AW, Corbett E, French PD, Zakrzewska JM. Oral mucosal leishmaniasis as a presenting feature of HIV infection and its management. *J Oral Pathol Med*. 1999;28:43–46.
22. Motta AC, Arruda D, Souza CS, Foss NT. Disseminated mucocutaneous leishmaniasis resulting from chronic use of corticosteroid. *Int J Dermatol*. 2003;42:703–706.
23. Tuon FF, Amato VS. Mucosal leishmaniasis and miltefosine. *Clin Infect Dis*. 2007;44:1525–1526.
24. Oleinick NL, Evans HH. The photobiology of photodynamic therapy: cellular targets and mechanisms. *Radiat Res*. 1998;150 Suppl 5: S146–S156.
25. van der Snoek EM, Robinson DJ, van Hellemond JJ, Neumann HA. A review of photodynamic therapy in cutaneous leishmaniasis. *J Eur Acad Dermatol Venereol*. 2008;22:918–922.
26. Triesscheijn M, Baas P, Schellens JH, Stewart FA. Photodynamic therapy in oncology. *Oncologist*. 2006;11:1034–1044.
27. Juzeniene A, Peng Q, Moan J. Milestones in the development of photodynamic therapy and fluorescence diagnosis. *Photochem Photobiol Sci*. 2007;6:1234–1245.
28. Allen CM, Sharman WM, van Lier JE. Current status of phthalocyanines in the photodynamic therapy of cancer. *J Porphyr Phthalocyanines*. 2001;5:161–169.
29. Owens JW, Smith R, Robinson M, Robins M. Photophysical properties of porphyrins, phthalocyanines and benzochlorins. *Inorg Chem Acta*. 1998;279:226–231.
30. Dysart JS, Patterson MS. Characterization of Photofrin photobleaching for singlet oxygen dose estimation during photodynamic therapy of MLL cells in vitro. *Phys Med Biol*. 2005;50:2597–2616.

31. Alexandratou E, Yova D, Loukas S. A confocal microscopy study of the very early cellular response to oxidative stress induced by zinc phthalocyanine sensitization. *Free Radic Biol Med*. 2005;39:1119–1127.
32. Chen R, Huang Z, Chen G, et al. Kinetics and subcellular localization of 5-ALA-induced PpIX in DHL cells via two-photon excitation fluorescence microscopy. *Int J Oncol*. 2008;32:861–867.
33. Li H, Jensen TJ, Fronczek FR, Vicente MG. Syntheses and properties of a series of cationic water-soluble phthalocyanines. *J Med Chem*. 2008;51:502–511.
34. Malham GM, Thomsen RJ, Finlay GJ, Baguley BC. Subcellular distribution and photocytotoxicity of aluminium phthalocyanines and haematoporphyrin derivative in cultured human meningioma cells. *Br J Neurosurg*. 1996;10:51–57.
35. Montanari J, Maidana C, Esteva MI, Salomon C, Morilla MJ, Romero EL. Sunlight triggered photodynamic ultradeformable liposomes against *Leishmania braziliensis* are also leishmanicidal in the dark. *J Control Release*. 2010;147:368–376.
36. Higa LH, Schilrreff P, Perez AP, et al. Ultradeformable archaeosomes as new topical adjuvants. *Nanomedicine*. 2012;8:1319–1328.
37. Gonzalez RO, Higa LH, Cutrullis RA, et al. Archaeosomes made of *Halorubrum tebenquichense* total polar lipids: a new source of adjuvancy. *BMC Biotechnol*. 2009;9:1–12.
38. Kates M, Kushwaha SC. Isoprenoids and polar lipids of extreme halophiles. In: Dassarma S, Fleischman EM, editors. *Archaea: A Laboratory Manual – Halophiles*. New York: Cold Spring Harbor Laboratory; 1995:35–54.
39. Bötcher CJF, Van Gent CM, Pries C. A rapid and sensitive sub-micro phosphorus determination. *Anal Chim Acta*. 1961;24:203–204.
40. Van den Bergh BA, Wertz PW, Junginger HE, Bouwstra JA. Elasticity of vesicles assessed by electron spin resonance, electron microscopy and extrusion measurements. *Int J Pharm*. 2001;217:13–24.
41. Inaba K, Inaba M, Romani N, et al. Generation of large numbers of dendritic cells from mouse bone marrow cultures supplemented with granulocyte/macrophage colony-stimulating factor. *J Exp Med*. 1992; 176:1693–1702.
42. Cevc G. Material transport across permeability barriers by means of lipid vesicles. In: Lipowsky R, Sackmann E, editors. *Handbook of Biological Physics*. Amsterdam: Elsevier; 1995:465–489.
43. Elsayed MM, Cevc G. The vesicle-to-micelle transformation of phospholipid-cholate mixed aggregates: a state of the art analysis including membrane curvature effects. *Biochim Biophys Acta*. 2011; 1808:140–153.
44. Carrer DC, Higa LH, Defain Tesoriero MV, Morilla MJ, Roncaglia DI, Romero EL. Structural features of ultradeformable archaeosomes for topical delivery of ovalbumin. *Colloids Surf B Biointerfaces*. In press 2014.
45. Boyle RW, Dolphin D. Structure and biodistribution relationships of photodynamic sensitizers. *Photochem Photobiol*. 1996;64:469–485.
46. Un K, Sakai-Kato K, Oshima Y, Kawanishi T, Okuda H. Intracellular trafficking mechanism, from intracellular uptake to extracellular efflux, for phospholipid/cholesterol liposomes. *Biomaterials*. 2012;33:8131–8141.
47. Gazi U, Martinez-Pomares L. Influence of the mannose receptor in host immune responses. *Immunobiology*. 2009;214:554–561.
48. Garrido VV, Dulgerian LR, Stempin CC, Cerbán FM. The increase in mannose receptor recycling favors arginase induction and *Trypanosoma cruzi* survival in macrophages. *Int J Biol Sci*. 2011;7:1257–1272.
49. Gordon S. Alternative activation of macrophages. *Nat Rev Immunol*. 2003;3:23–35.
50. Mosser DM. The many faces of macrophage activation. *J Leukoc Biol*. 2003;73:209–212.
51. Mosser DM, Edwards JP. Exploring the full spectrum of macrophage activation. *Nat Rev Immunol*. 2008;8:958–969.
52. Jaafari MR, Bavarsad N, Fazly Bazzaz BS, et al. Effect of topical liposomes containing paromomycin sulfate (PM) in the course of *Leishmania major* infection in susceptible BALB/c mice. *Antimicrob Agents Chemother*. 2009;53:2259–2265.
53. Bavarsad N, Fazly Bazzaz BS, Khamesipour A, Jaafari MR. Colloidal, in vitro and in vivo anti-leishmanial properties of transfersomes containing paromomycin sulfate in susceptible BALB/c mice. *Acta Tropica*. 2012;124:33–41.
54. Akilov OE, Kosaka S, O'Riordan K, Hasan T. Parasiticidal effect of δ-aminolevulinic acid-based photodynamic therapy for cutaneous leishmaniasis is indirect and mediated through the killing of the host cells. *Exp Dermatol*. 2007;16:651–660.
55. Kosaka S, Akilov OE, O'Riordan K, Hasan T. A mechanistic study of δ-aminolevulinic acid-based photodynamic therapy for cutaneous leishmaniasis. *J Invest Dermatol.* 2007;127:1546–1549.
56. Taylor VM, Cedeño DL, Muñoz DL, et al. In vitro and in vivo studies of the utility of dimethyl and diethyl carbaporphyrin ketals in treatment of cutaneous leishmaniasis. *Antimicrob Agents Chemother*. 2011;55:4755–4764.
57. Hernández IP, Montanari J, Valdivieso W, Morilla MJ, Romero EL, Escobar P. In vitro phototoxicity of ultradeformable liposomes containing chloroaluminum phthalocyanine against New World *Leishmania* species. *J Photochem Photobiol B*. 2012;117:157–163.
58. Akilov OE, Kosaka S, O'Riordan K, Hasan T. Photodynamic therapy for cutaneous leishmaniasis: the effectiveness of topical phenothiaziniums in parasite eradication and Th1 immune response stimulation. *Photochem Photobiol Sci*. 2007;6:1067–1075.
59. Dutta S, Ray D, Kolli BK, Chang KP. Photodynamic sensitization of *Leishmania amazonensis* in both extracellular and intracellular stages with aluminum phthalocyanine chloride for photolysis in vitro. *Antimicrob Agents Chemother*. 2005;49:4474–4484.
60. Chen X, Zhong Z, Xu Z, Chen L, Wang Y. 2′,7′-Dichlorodihydrofluorescein as a fluorescent probe for reactive oxygen species measurement: forty years of application and controversy. *Free Radic Res*. 2010;44:587–604.